metals

MDPI

Article

The Effect of Cathodic Cage Plasma TiN Deposition on Surface Properties of Conventional Plasma Nitrided AISI-M2 Steel

Luiz Henrique Portela de Abreu [1], Muhammad Naeem [2,*], Renan Matos Monção [1], Thercio H. C. Costa [3], Juan C. Díaz-Guillén [4], Javed Iqbal [5,6] and Rômulo Ribeiro Magalhães Sousa [1,7]

1 Advanced Materials Interdisciplinary Laboratory (LIMAV), Postgraduate Program in Materials Science and Engineering, Federal University of Piaui (UFPI), Teresina 64000-000, PI, Brazil; luizhabreu92@gmail.com (L.H.P.d.A.); renanmatos2010@hotmail.com (R.M.M.); romulorms@gmail.com (R.R.M.S.)
2 Department of Physics, Women University of Azad Jammu and Kashmir, Bagh 12500, Pakistan
3 Mechanical Department, Federal University of Rio Grande do Norte (UFRN), Natal 59000-000, RN, Brazil; thercioc@gmail.com
4 CONACYT-Corporación Mexicana de Investigación en Materiales, Saltillo 25290, Mexico; jcarlos@comimsa.com
5 Department of Physics, University of Azad Jammu and Kashmir, Muzaffarabad 13100, Pakistan; javedkiqbal@gmail.com
6 Department of Physics and Astronomy, University of Latvia, Raina bulvaris 19, LV-1586 Riga, Latvia
7 Mechanical Departament, Federal University of Piaui (UFPI), Teresina 64000-000, PI, Brazil
* Correspondence: mnaeem@wuajk.edu.pk

check for updates

Citation: de Abreu, L.H.P.; Naeem, M.; Monção, R.M.; Costa, T.H.C.; Díaz-Guillén, J.C.; Iqbal, J.; Sousa, R.R.M. The Effect of Cathodic Cage Plasma TiN Deposition on Surface Properties of Conventional Plasma Nitrided AISI-M2 Steel. *Metals* **2022**, *12*, 961. https://doi.org/10.3390/met12060961

Academic Editors: Shinichiro Adachi, Francesca Borgioli, Thomas Lindner and Marcello Cabibbo

Received: 9 May 2022
Accepted: 31 May 2022
Published: 2 June 2022

Publisher's Note: MDPI stays neutral with regard to jurisdictional claims in published maps and institutional affiliations.

Abstract: In this study, a combination of conventional plasma nitriding and cathodic cage plasma deposition (CCPD) at different temperatures (400 and 450 °C) is implemented to enhance the surface properties of AISI-M2 steel. This combination effectively improves the surface hardness and the formation of a favorable hardness gradient toward the core, which would benefit the load-bearing capacity of substrate. The duplex-treated samples exhibit iron nitrides (Fe_4N, $Fe_{2-3}N$) and titanium nitride (TiN) phases. The thickness of the hard-TiN layer is 1.35 and 2.37 µm, whereas the combined thickness of the hard film and diffusion layer is 87 and 124 µm, for treatment at 400 and 450 °C, respectively. The wear rate and friction coefficient are dramatically reduced by duplex treatment. The oxidative wear mechanism and adhesive wear mechanism are dominant for duplex-treated samples. This study suggests that the cathodic cage plasma deposition technique can attain a combination of hard film and diffusion layer. The plasma nitriding before CCPD is beneficial for attaining an adequate nitrogen diffusion layer thickness. The drawbacks of conventional TiN film deposition, such as "egg-shell" problems, can be removed.

Keywords: cathodic cage plasma deposition; hardness; wear resistance; titanium nitride

1. Introduction

AISI-M2 is molybdenum-containing high-speed steel widely used in several cold work applications such as punching, pressing, and forming tools. The performance of high-speed steel tools can be upgraded by surface modification either by thermochemical diffusion techniques or the deposition of hard coatings. As a result, the machining performance of tools can be increased, reducing personnel cost and maintenance expenditure [1].

Among thermochemical diffusion techniques, plasma nitriding is widely applied to enhance the tribo-mechanical properties of tool steels by altering their microstructure [2]. In this process, nitrogen atoms are diffused in the surface and near-surface zone, and thus, surface mechanical and tribological properties are changed. Commonly, the nitrided steel contains a compound zone (white layer) and diffusion zone [3,4]. The white layer contains iron nitrides formed on the top surface of the nitrided sample, while the diffusion zone is due to interstitially dissolved nitrogen atoms or precipitated iron nitrides [3]. The presence

of a white layer can improve the surface hardness of tool steel, but it is not beneficial for tribological properties. The white layer is brittle, and thus it is cracked down during sliding contact, generating hard abrasive particles on the sliding path, and thus it can damage the wear resistance [5,6]. White layer formation, which is unsuitable for industrial application, can be avoided by fine-tuning control parameters such as temperature, gas composition, and treatment time [7]. On the other hand, hard film deposition such as titanium nitride by physical vapor deposition (PVD) or chemical vapor deposition (CVD) is used to improve the surface properties of steel. TiN coating exhibits high hardness, low friction coefficient, and superior wear resistance [8–10]. Unfortunately, such hard coatings have poor adhesion with the substrate due to a significant difference in hardness between coating and substrate [11]. Thus, the combination of the thermochemical diffusion technique and hard film deposition is beneficial.

In the conventional plasma-nitriding (CPN) technique, the substrate is kept at the cathodic potential, and the reactor body acts as an anode. Its working is based on the sputtering re-deposition model [12]: the bombardment of incident ions on cathodic samples, removal of sample material, and reaction with nitrogen gas in plasma to form iron nitrides. These nitrides are re-condensed on the sample's surface, and nitrogen atoms subsequently diffuse in the sample. Here, sample material is sputtered and re-deposited, and thus, only nitrides of sample materials can be formed. Approximately two decades ago [13,14], the cathodic cage plasma-nitriding technique (CCPN) was introduced. In CCPN, samples are kept at floating potential and covered with a cathodic metallic screen (active screen or cathodic cage) [13]. Ions directly bombard the cathodic cage, and the material of the cathodic cage is sputtered and re-deposited on the surface of the sample. Thus, nitrides of any material can also be deposited on samples, and due to this fact, it is referred to as cathodic cage plasma deposition (CCPD). This method is widely used to deposit numerous materials such as iron, chromium, aluminum, nickel, niobium, copper, silver, and titanium [15–19]. As in cathodic cage plasma deposition, simultaneous diffusion of nitrogen atoms and deposition of cage material occurs, and thus, it is predicted to be more valuable to deposit titanium nitride hard film.

Several authors reported the duplex treatment (plasma nitriding and TiN film deposition) on steel samples [20–22]. They found that duplex treatment can create a hardness gradient among TiN film and sample, and thus adhesion of hard film can be enhanced. However, they used PVD, CVD techniques for TiN film deposition, and a separate system is required for nitriding and TiN film deposition. Thus, this combination is relatively expensive. Besides this, the TiN film has low adhesion with substrate and shows an "egg-shell" problem [23].

In this study, samples are nitrided by the CPN technique, and subsequently, TiN is deposited by the CCPD technique. First, the samples are initially nitrided by CPN to create an effective diffusion zone [8] and a hardness gradient before deposition of TiN. Then, the TiN is deposited on pre-nitrided samples at different temperatures, 400 °C and 450 °C, by the CCPD technique.

2. Experimental Details

AISI-M2 high-speed steel sample (nominal composition provided in Table 1 with a cylindrical geometry (diameter 2 cm and thickness 1 cm) were considered. Before plasma treatment, samples were polished using silicon carbide papers of multiple sizes (300–2500). Then, they were mirror polished with alumina powder, cleaned in an ultrasonic bath, and rinsed in flowing water.

Table 1. Chemical composition (wt.%) of AISI-M2 high-speed steel samples.

Si	Mn	Co	W	V	Mo	Cr	C	Fe
0.45	0.3	1	6.1	1.9	5	4.1	0.8	Balance

The CPN treatment was carried out in a laboratory-scale plasma-nitriding reactor made of austenitic stainless steel (304) with a cylindrical shape having 30 cm diameter and 30 cm height. The reactor's body was grounded, which works as an anode, whereas the sample holder works as a counter electrode (cathode). The power of 400 W is kept constant during processing. The details of a CPN reactor are described elsewhere [24]. The titanium nitride is deposited by a CCPD system equipped with a titanium cathodic cage. This system is developed by covering the cathodic base plate of CPN with a titanium cathodic cage and keeping samples on the ceramic insulator plate [24]. The cathodic cage was biased with a high-voltage source (2 A and 1200 V). The cathodic cage comprises two concentric cylinders. The inner cylinder is 35 mm in height and 45 mm in diameter, and the outer cylinder is 45 mm in height and 65 mm in diameter, as described earlier [25]. The samples are first treated by CPN to create an effective diffusion layer and subsequently treated by CCPD to deposit a hard titanium nitride layer. Thus, this combination of treatments is named duplex plasma treatment. The labeling of samples and detailed processing conditions are given in Table 2.

Table 2. Labelling of samples and corresponding treatment conditions.

Conventional Plasma Nitriding				Cathodic Cage Plasma Deposition				Sample Labeling
Gases (sccm)	**Pressure (Pa)**	**Time (h)**	**Temperature (°C)**	**Gases (sccm)**	**Pressure (Pa)**	**Time (h)**	**Temperature (°C)**	
Quenching and tempering								Base
30 H_2_10N_2	350	4	400					CPN
30 H_2_10N_2	350	4	400	30 H_2 _ 10N_2	350	4	400	Duplex 400
30 H_2_10N_2	350	4	400	30 H_2 _ 10N_2	350	4	450	Duplex 450

The X-ray diffraction (XRD) data were obtained by an X-ray diffractometer (Malvern Panalytical LTD, Malvern , UK)Empyrean, radiation Cu-Kα (λ = 1.54 Å)) operated with a copper target tube at a voltage of 45 kV, current of 40 mA, scanning angle of (2θ) from 30° to 90°, and a stepping angle of 0.013°. It was equipped with Soller slits, which consist of large numbers of parallel plates in the plane of diffraction to limit the spread of incident and diffracted X-ray beams. Additionally, it contained graded multilayer Goebel mirrors. The phases formed on the near-surface zone and deep inside the sample were assessed by grazing incidence (0.3, 1, 3, and 5°) and conventional X-ray diffraction, respectively. The XPert High Score Plus software was used for the phase's identification. The microhardness of samples was evaluated by a Vickers microhardness tester. The equipment used to perform the microhardness testing was a Shimadzu microhardness tester (model HMV 2000). The load used in each analysis was 50 gf. For the superficial microhardness analysis, 10 indentations were made along the sample surface, while for the preparation of the microhardness profile along with the nitrided layer, the samples were cut, sanded with silicon carbide papers, embedded in resin, and indentations were made along its cross-section in a total of 8 indentations. The surface and cross-sectional scanning electron microscope (SEM) analyses were carried out by Tescan Mira 3, operated with 12 kV voltage. The titanium composition in films was assessed by energy dispersive spectroscopy (EDS) (Bruker, model X flash, Billerica, MA, USA). The EDS analysis was performed by 15 kV accelerating voltage over 100 s. The presence of nitrogen in deposited films was examined by wavelength-dispersive spectroscopy (WDS) [26]. The WDS conditions were 20 kV beam voltage, 14.5 µm work distance, dwell time of 2.5 s, and beam intensity close to 20 nA. For nitrogen analysis, a Bruker detector with Crystal BRML80-Ka1 signal was used. Optical microscopy was also used in the cross-sectional observation of deposited layers. The wear resistance was assessed by a ball-on-disc wear tester containing a SiC ball of 6 mm diameter and a normal load of 1 N. A sliding speed of 5 cm/s and wear track radius of 7 mm were used.

3. Results and Discussion

The hardness profiles of base material (quenched and tempered as described elsewhere [27]) and conventional plasma-nitrided (CPN) and duplex-treated samples (base sample is first treated in CPN, and then TiN is deposited by CCPD at 400 °C and 450 °C) are shown in Figure 1. The first point in the hardness profile corresponds to the hardness on the sample's surface. It shows that the hardness of the base sample (~590 $HV_{0.05}$) increases up to 1000, 1467, and 1716 $HV_{0.05}$ for the CPN sample and duplex-treated samples at 400 °C and 450 °C, respectively. Thus, the hardness is improved by duplex treatment and is significantly higher than only nitrided M2 steel samples. In addition, the hardness profile shows an increase up to a higher depth. Our results show that a favorable hardness gradient is formed along with the sample's depth, which can be ascribed to the diffusion of nitrogen atoms up to higher depth during CPN and subsequent diffusion during CCPD. This can be further confirmed by the cross-sectional SEM analysis presented later.

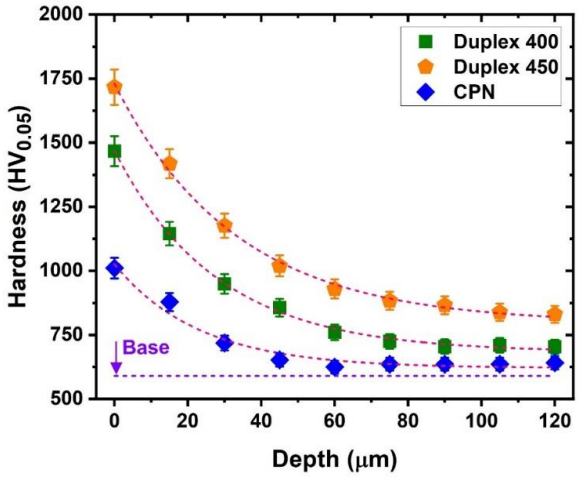

Figure 1. Hardness profile of conventional plasma-nitrided (CPN) and duplex-treated samples with substrate temperature for TiN deposition at 400 °C and 450 °C.

The conventional X-ray diffraction pattern of a base sample and CPN and duplex-treated samples at 400 °C and 450 °C is plotted in Figure 2. The base material (Figure 2a) comprises two phases: martensite, and carbide. The α-Fe martensite phase appears from the steel matrix, whereas the carbide phase (M6C) comes from the combination of alloying elements (where M = Mo, W, Cr, V) with carbon [28]. The M6C carbide phase has a face-centered cubic (FCC) structure [29]. The nitrided sample (Figure 2b) shows the presence of iron nitrides Fe_4N (COD: 96-900-4226) and $Fe_{2-3}N$ (96-152-5732) phases. The samples nitrided in CPN and TiN-deposited by CCPD show (Figure 2c,d) the presence of iron nitrides Fe_4N (COD: 96-900-4226) and $Fe_{2-3}N$ (96-152-5732) and less intense peaks of titanium nitride TiN (96-101-1101). However, it is quite challenging to identify the phases of nitrided M2 steel due to the formation of nitrides of substrate alloying elements and conversion of carbides (primary and secondary) into carbo-nitrides—or only nitrides—as reported in the literature [28]. The phases of many nitrides appear close to the carbides, and thus, diffraction peaks of nitrides are not distinguishable and overlap. Thus, the intensity of background peaks is enhanced [28]. This change in intensity and broadness of background peaks reveals the formation of iron nitrides in addition to background peaks. As nitrided samples are post-treated by Ti cathodic cage, the peaks corresponding to TiN are less intense. This shows that a thin TiN layer is formed. Thus, the film is characterized by grazing incidence XRD using different incident angles 0.3–5°, as presented in Figure 3. The top layer is mainly composed of TiN, and no intense background peaks corresponding to iron or alloying element nitrides appear. However, when shifting to the core of the sample (higher incidence angles), alloying element carbides and iron nitrides appear again. While comparing the intensity of background peaks at the same incidence angle, at 400 °C,

peaks are more intense than at 450 °C. This reveals that a thicker TiN layer is formed in this condition, confirmed by cross-sectional SEM analysis. No intense peaks corresponding to Ti or Ti_2N are observed; thus, the deposited films are stoichiometric. The mechanism behind the formation of TiN by CCPD can be ascribed to the well-known mechanisms of CCPN. The working principles of both CCPN and CCPD are similar, and models proposed for CCPN can be applied to CCPD. The only difference in these systems is that under a certain processing pressure range, the additional hollow cathode effect arises through the holes of the cathodic cage, which can increase the intensity of discharge [30]. As proposed in several models, such as Saeed et al. [31], Hubbard et al. [32], Gallo et al. [33], and Fraczek et al. [34], primarily energetic ions sputter titanium atoms from the cathodic cage, subsequently react with active nitrogen atoms, and form nitrides of metal atoms, such as TiN in this case. These nitrides are re-deposited on the substrate, and afterward, nitrogen atoms are diffused in the substrate.

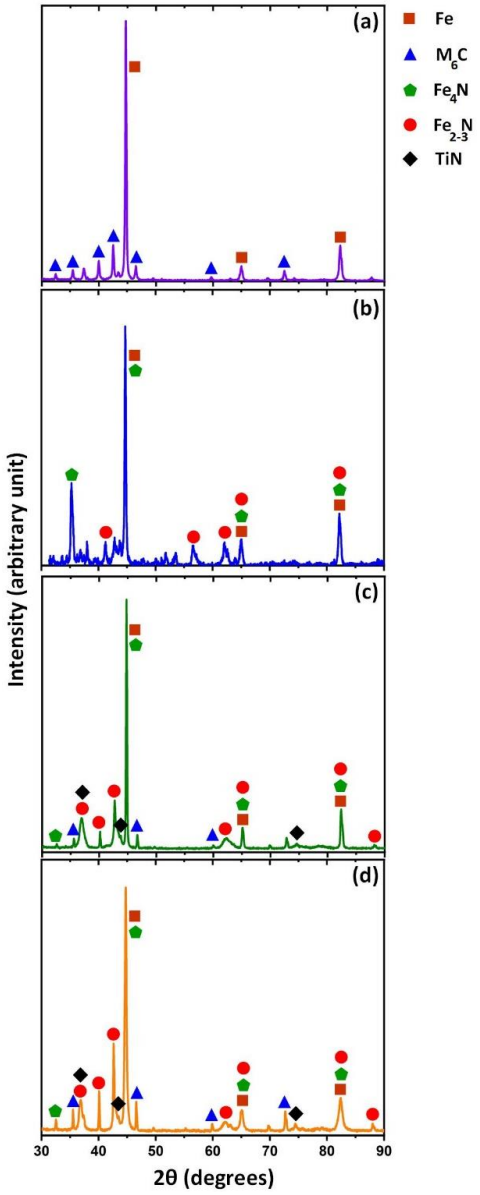

Figure 2. Conventional X-ray diffraction of (**a**) base sample, (**b**) CPN, and duplex-treated samples with substrate temperature for TiN deposition at (**c**) 400 °C and (**d**) 450 °C.

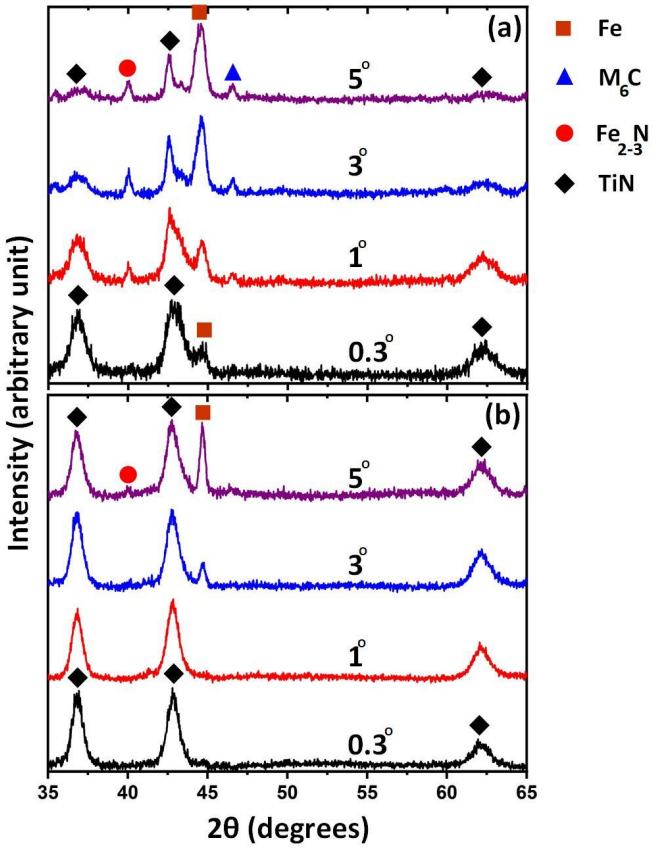

Figure 3. Grazing incidence X-ray diffraction of duplex-treated samples with substrate temperature for TiN deposition at (**a**) 400 °C and (**b**) 450 °C.

The surface SEM images of base material and nitrided and duplex-treated samples are shown in Figure 4. The base surface (Figure 4a) contains polishing scratches induced by the mechanical polishing of samples before plasma processing. The surface of the nitrided sample (Figure 4b) contains uniformly distributed polygonal iron nitride particles, following the literature [7]. The surface of the duplex-treated samples (Figure 4c,d) contains uniformly dispersed spherical nanoparticles agglomerated to coralloid granular nitrides, as shown in high-resolution images. These particles are mainly composed of Ti and N elements observed by EDS analysis (spectra are not presented here). The particles are more agglomerated for the sample treated at higher temperatures [35]. The deposition of Ti can be ascribed to the cathodic cage sputtering and its re-deposition on the substrate.

The thickness of the deposited layer is assessed by cross-sectional optical microscopy, as presented in Figure 5a,b,d. It reveals thicknesses of 71 µm, 98 µm, and 124 µm for nitrided and duplex-treated samples at 400 °C and 450 °C. The thickness increases with processing temperature due to better diffusion of nitrogen atoms in the steel matrix. This layer thickness is the combined thickness of the TiN and diffusion layer, and layers are not distinguishable due to resolution limitations. Therefore, the samples were further etched to observe the TiN layer and observed by high-resolution cross-sectional SEM analysis, as presented in Figure 5c,e. The titanium nitride layer in the top zone is confirmed by titanium elemental mapping, as presented in Figure 5b. This shows that the thickness of the TiN layer is 1.35 µm and 2.37 µm for treatment at 400 °C and 450 °C, respectively. The increase in thickness of TiN layer with temperature might be due to the higher sputtering from the cathodic cage [36]. The typical EDS spectrum of duplex-treated samples with TiN deposition at 400 °C is shown in Figure 6, which shows the presence of Ti and N on the surface. This is further clarified by cross-sectional elemental line scan analysis and WDS, as presented in Figure 7. This shows that titanium is mainly present in the top region of treated samples and is quite comparable to the thickness of the TiN layer measured by

cross-sectional SEM images. However, nitrogen is presented up to a higher depth due to the diffusion during the pre-nitriding process and CCPD. This diffusion of nitrogen atoms to a higher depth is the cause of the hardness gradient between a sample and its TiN layer, and thus, this film is predicted to be valuable for wear resistance. Usually, in conventional techniques, the titanium nitride layer is not so adhesive with the substrate, and it can be avoided by CCPD. Additionally, the pre-nitriding process is responsible for effective diffusion zone production, and thus, a better hardness gradient with the substrate can be produced, as observed in Figure 1.

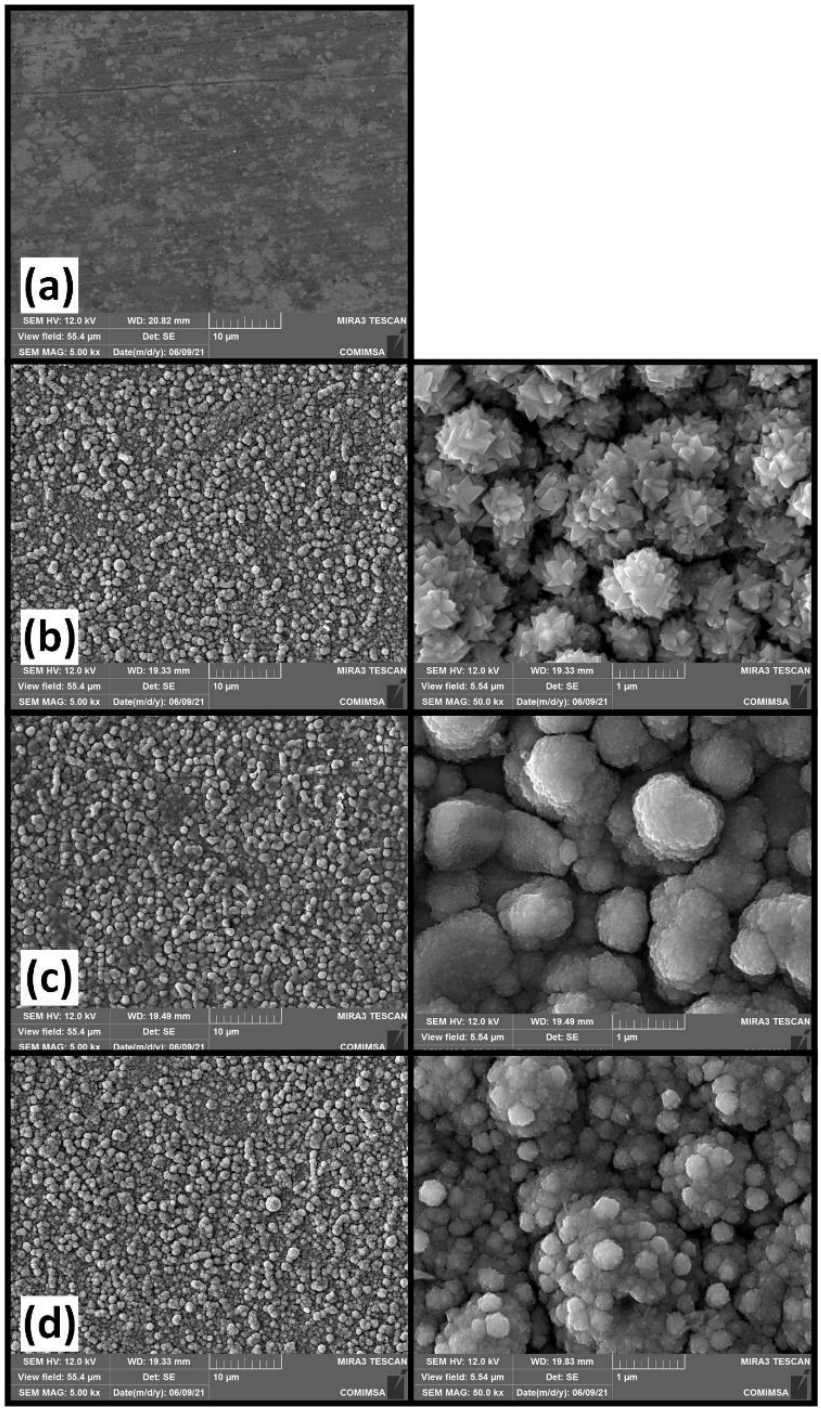

Figure 4. SEM micrographs of (**a**) base sample and (**b**) CPN and duplex-treated samples with substrate temperature for TiN deposition at (**c**) 400 °C and (**d**) 450 °C.

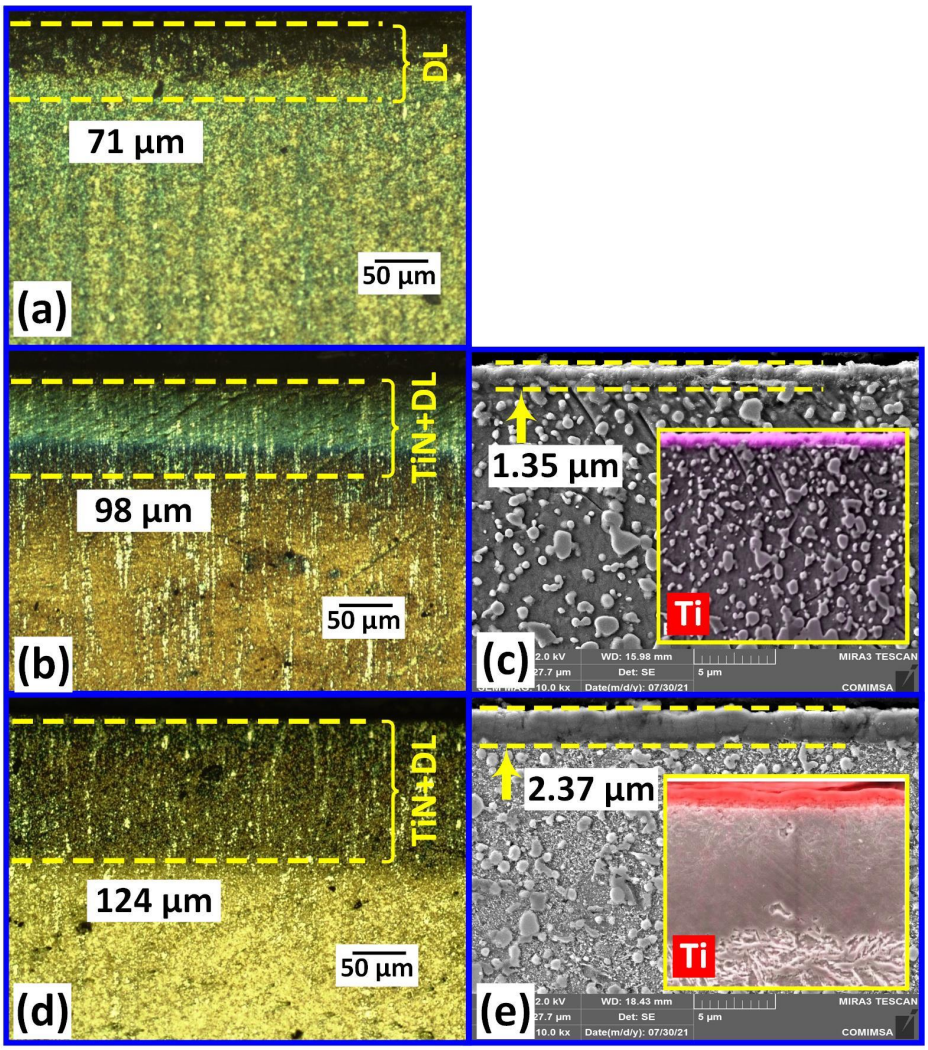

Figure 5. Cross-sectional optical micrograph of (**a**) nitrided sample, optical micrographs with SEM images of duplex-treated samples with substrate temperature for TiN deposition at (**b**,**c**) 400 °C and (**d**,**e**) 450 °C.

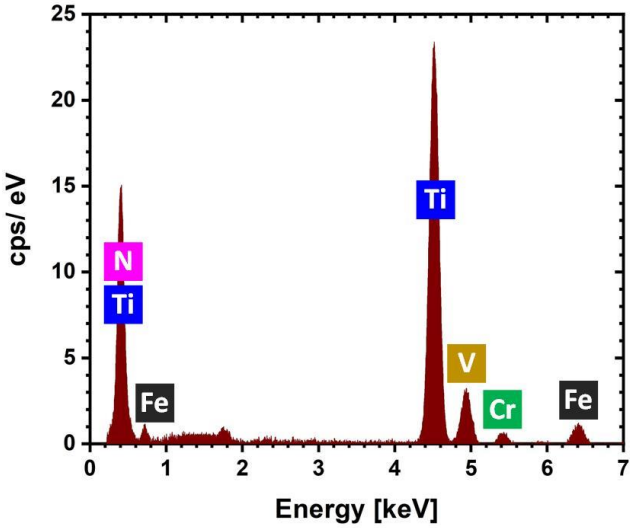

Figure 6. Typical EDS spectrum of duplex-treated samples with TiN deposition temperature of 400 °C.

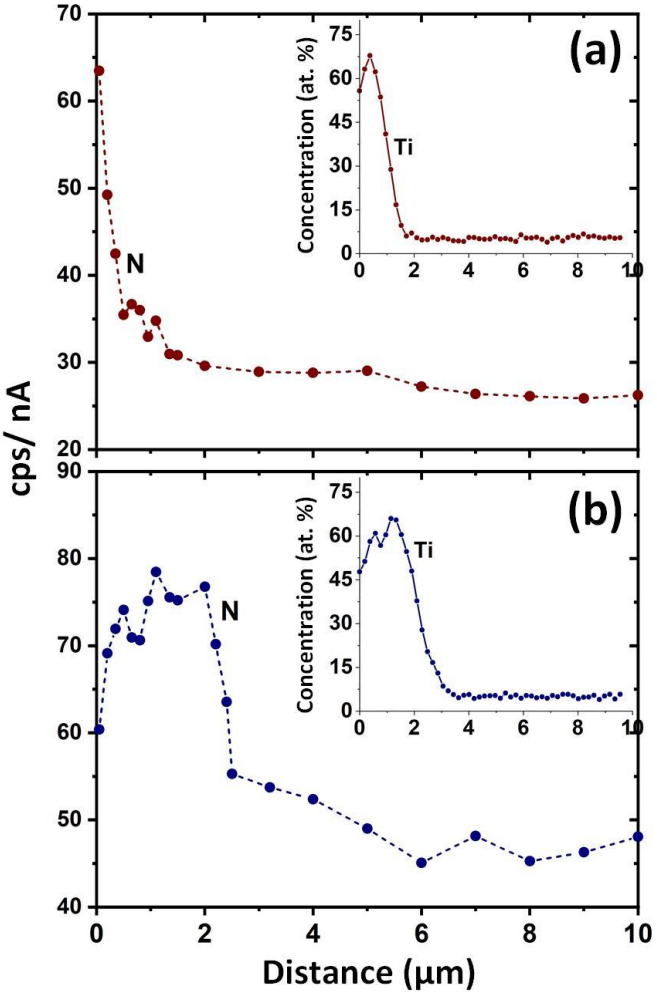

Figure 7. WDS profile (for N detection) and EDS line scan (for Ti detection) of duplex-treated samples with substrate temperature for TiN deposition at (**a**) 400 °C and (**b**) 450 °C.

The performance of deposited films in sliding contact parts applications is assessed by a ball-on-disc wear tester and worn tracks SEM images are presented in Figure 8. It shows that base sample (Figure 8a) is severely worn, and tracks are wider than treated samples. The abrasion grooves appear, and the surface contains metallic debris and microcracks. These grooves and microcracks appear due to the low hardness of the base material, and thus, micro-ploughing and plastic deformation is induced during sliding contact of the ball. The tracks show that the abrasive wear mechanism contributes to the base sample. The worn track of the nitrided sample (Figure 8b) is relatively narrow and smoother than the base material due to increased hardness and resistance to plastic deformation. The duplex-treated sample's surface in Figure 8c,d shows that the surface is smooth—free of cracks and metallic debris. This shows the existence of an adhesive wear mechanism. The surface is hard enough for treated samples to prevent plastic deformation during sliding contact against the ball. The oxygen elemental mapping reveals that the track is oxidized, and an oxidative wear mechanism is also present. The titanium elemental mapping shows that the entire surface of the sample, including the worn surface, contains homogeneous titanium distribution. The titanium nitride layer is not removed during sliding contact against the ball. This is primarily due to the hybrid mechanism of CCPD, which involves the deposition of titanium, and the thermochemical diffusion process. This hybrid mechanism produces TiN film with good adherence to the substrate. Additionally, the plasma pre-nitriding process also produces an effective diffusion layer, increasing adhesion with the substrate. Thus, the wear resistance is increased by duplex plasma treatment.

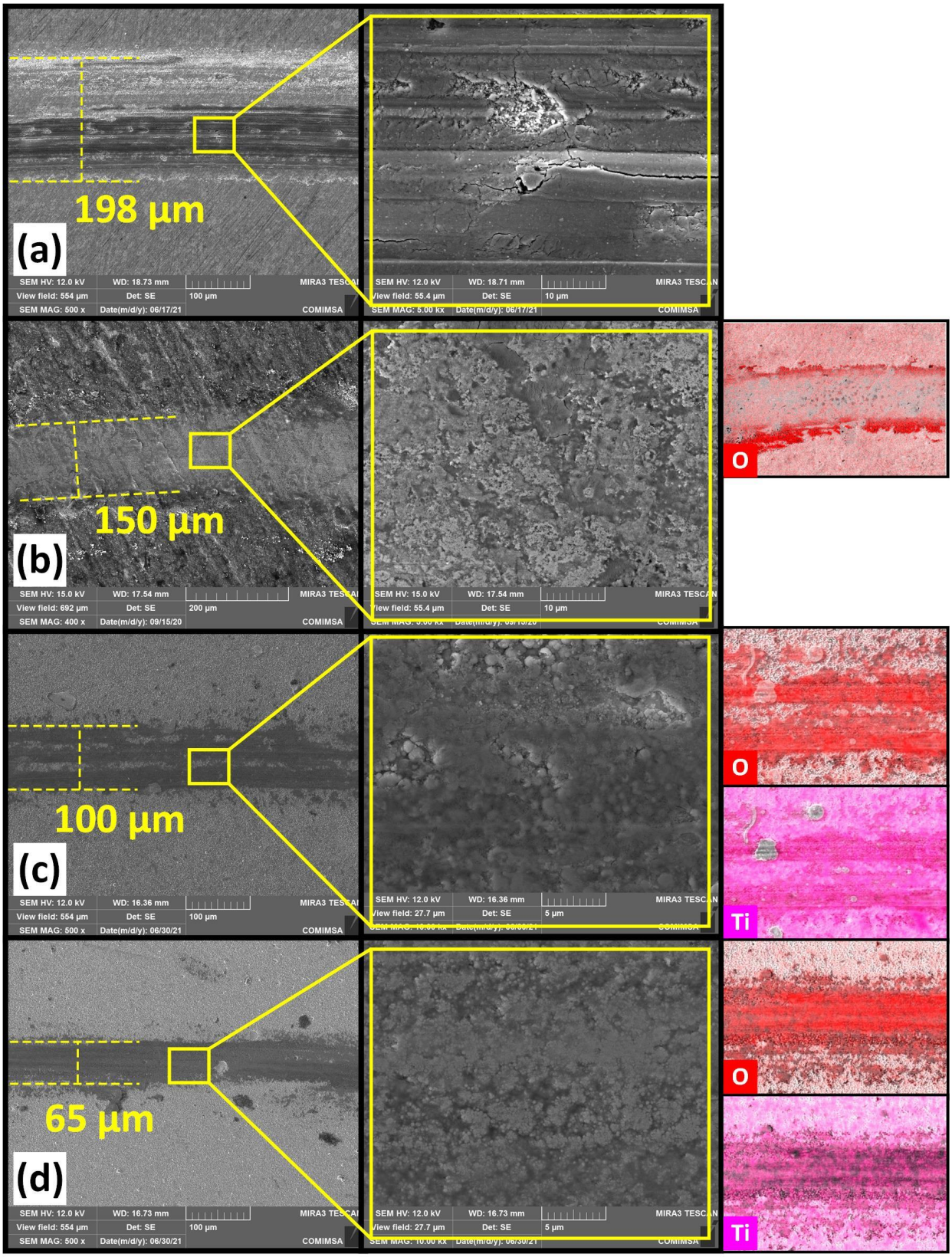

Figure 8. SEM images along with corresponding elemental mapping of (**a**) base sample and (**b**) CPN and duplex-treated samples with substrate temperature for TiN deposition at (**c**) 400 °C and (**d**) 450 °C.

The friction coefficients of the base material and nitrided and duplex-plasma-treated samples with sliding distance are compared in Figure 9, and corresponding averages are plotted in Figure 10. The friction coefficient of the base material fluctuates with the sliding distance, and average values are higher than the treated samples. This can be ascribed to the low hardness of the base sample, and thus, severe wear as described earlier [37]. The variation of friction coefficient with change in sliding distance is probably caused by the formation and subsequent removal of the oxide layer on further sliding [37]. This is supported by the surface SEM image of the base sample, in which bright and dark regions appear due to oxidation of the surface and later spalling. The friction coefficient of treated samples shows relatively smooth and low values due to sufficient hardness and low wear rate of treated samples. This is also supported by surface SEM images, in which the surface of treated samples is smooth, clean, and free of imperfection. The wear rates of the base sample and nitrided and duplex-treated samples are compared in Figure 10. This shows a significant decrease in wear rate by duplex plasma treatment due to sufficient hardness of the sample and sufficient adhesion with the substrate, due to which hard TiN film is not detached from the substrate during sliding contact.

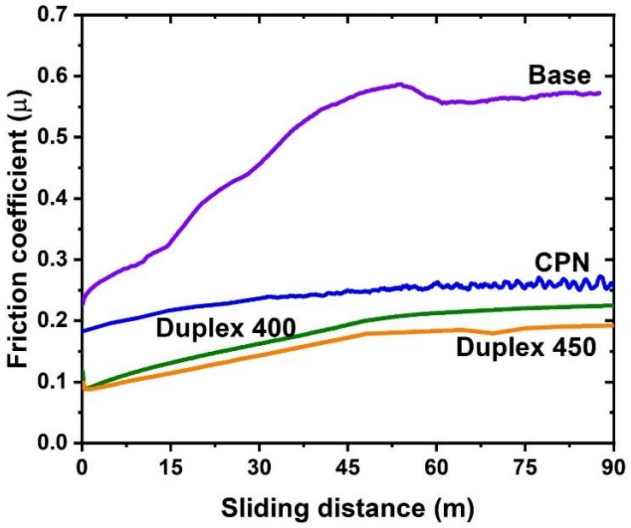

Figure 9. Variation of friction coefficient with sliding distance of base sample, CPN, and duplex-treated samples with substrate temperature for TiN deposition at 400 °C and 450 °C.

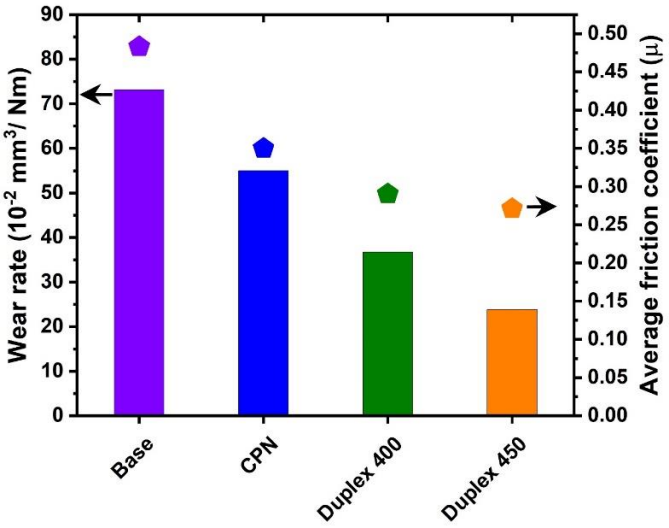

Figure 10. Wear rate and average friction coefficient of base sample and CPN and duplex-treated samples with substrate temperature for TiN deposition at 400 °C and 450 °C.

4. Conclusions

Nitriding of AISI-M2 steel is carried out in a conventional plasma nitriding system and subsequently, cathodic cage plasma deposition with a titanium cage is used to improve surface properties. The hardness of the base sample (590 $HV_{0.05}$) is increased by duplex treatment, and the maximum hardness of ~1716 $HV_{0.05}$ is attained by cathodic cage plasma deposition at 450 °C. Besides the increase in surface hardness, a favorable hardness gradient with depth is obtained by duplex treatment due to the formation of the diffusion layer during plasma nitriding as well as cathodic cage plasma deposition. The grazing-incidence-angle X-ray diffraction depicts titanium nitride formed on the nitrided sample during CCPD. The combined thicknesses of titanium nitride and diffusion layer are 87 and 124 µm for samples treated at 400 °C and 450 °C, respectively. The individual thickness of the titanium nitride layer is 1.53 µm and 2.37 µm. Furthermore, duplex treatment reduces the wear rate and friction coefficient significantly due to the formation of the hard titanium nitride layer in the near-surface zone and favorable hardness gradient, which increases hard film adhesion with the substrate. As a result, the wear tracks are relatively narrower and shallower for treated samples and adhesive, and the oxidative wear mechanism is dominant for treated samples in contrast with abrasive and oxidative wear in the base sample.

Author Contributions: Conceptualization, M.N., L.H.P.d.A., R.R.M.S., Methodology, R.M.M., T.H.C.C., J.C.D.-G., writing orignal draft, M.N., Writing review and editing, J.C.D.-G., R.M.M. and J.I. Supervision, R.R.M.S., T.H.C.C., Formal analysis, J.I., R.M.M., J.C.D.-G. All authors have read and agreed to the published version of the manuscript.

Funding: This study was financed in part by the "Coordenação de Aperfeiçoamento de Pessoal de Nível Superior (CAPES), Brazil" Finance Code 001. L. Henrique is thankful to "Universidade Federal do Piaui"and "Instituto Federal do Amazonas" for partial financial support in this research work. Javed Iqbal is thankful to European Regional Development Fund (Project No. 1.1.1.5/19/A/003) for the development of quantum optics and photonics lab at the university of Latvia.

Institutional Review Board Statement: Not applicable.

Informed Consent Statement: Not applicable.

Data Availability Statement: All data generated or analyzed during this study are included in this published article.

Conflicts of Interest: The authors declare no conflict of interest.

References

1. Libório, M.S.; Praxedes, G.B.; Lima, L.L.F.; Nascimento, I.G.; Sousa, R.R.M.; Naeem, M.; Costa, T.H.; Alves, S.M.; Iqbal, J. Surface modification of M2 steel by combination of cathodic cage plasma deposition and magnetron sputtered MoS_2-TiN multilayer coatings. *Surf. Coat. Technol.* **2020**, *384*, 125327. [CrossRef]
2. Nascimento, I.O.; Naeem, M.; Freitas, R.S.; Nascimento, R.M.; Viana, B.C.; Sousa, R.R.M.; Feitor, M.C.; Iqbal, J.; Costa, T.H.C. Comparative study of structural and stoichiometric properties of titanium nitride films deposited by cathodic cage plasma deposition and magnetron sputtering. *Eur. Phys. J. Plus* **2022**, *137*, 319. [CrossRef]
3. daS Rocha, A.; Strohaecker, T.; Hirsch, T. Effect of different surface states before plasma nitriding on properties and machining behavior of M2 high-speed steel. *Surf. Coat. Technol.* **2003**, *165*, 176–185. [CrossRef]
4. Bonu, V.; Srinivas, G.; Kumar, V.P.; Joseph, A.; Narayana, C.; Barshilia, H.C. Temperature dependent erosion and Raman analyses of arc-deposited H free thick DLC coating on Cr/CrN coated plasma nitrided steel. *Surf. Coat. Technol.* **2022**, *436*, 128308. [CrossRef]
5. Das, K.; Alphonsa, J.; Ghosh, M.; Ghanshyam, J.; Rane, R.; Mukherjee, S. Influence of pretreatment on surface behavior of duplex plasma treated AISI H13 tool steel. *Surf. Interfaces* **2017**, *8*, 206–213. [CrossRef]
6. Alsaran, A.; Altun, H.; Karakan, M.; Celik, A. Effect of post-oxidizing on tribological and corrosion behaviour of plasma nitrided AISI 5140 steel. *Surf. Coat. Technol.* **2004**, *176*, 344–348. [CrossRef]
7. Díaz-Guillén, J.C.; Naeem, M.; Hdz-García, H.M.; Acevedo-Davila, J.L.; Díaz-Guillén, M.R.; Khan, M.A.; Iqbal, J.; Mtz-Enriquez, A.I. Duplex plasma treatment of AISI D2 tool steel by combining plasma nitriding (with and without white layer) and post-oxidation. *Surf. Coat. Technol.* **2020**, *385*, 125420. [CrossRef]
8. Balashabadi, P.; Larijani, M.M.; Shokri, A.A.; Jafari-Khamse, E.; Seyedi, H.; Eshghi, S. The effect of bias voltage on microstructure and hardness of TiN films grown by ion coating deposition. *Eur. Phys. J. Plus* **2015**, *130*, 1–10. [CrossRef]

9. Guha, S.; Das, S. Investigation over effect of different carbon content on various properties of titanium carbon nitride (TiCN) coating grown on Si (100) substrate by chemical vapor deposition (CVD) process. *Eur. Phys. J. Plus* **2022**, *137*, 363. [CrossRef]
10. Smagoń, K.; Stach, S.; Ţălu, Ş.; Arman, A.; Achour, A.; Luna, C.; Ghobadi, N.; Mardani, M.; Hafezi, F.; Ahmadpourian, A.; et al. Studies of the micromorphology of sputtered TiN thin films by autocorrelation techniques. *Eur. Phys. J. Plus* **2017**, *132*, 1–15. [CrossRef]
11. Libório, M.S.; Almeida, E.O.; Alves, S.M.; Costa, T.H.C.; Feitor, M.C.; Nascimento, R.M.; Sousa, R.R.M.; Naeem, M.; Jelani, M. Enhanced surface properties of M2 steel by plasma nitriding pre-treatment and magnetron sputtered TiN coating. *Int. J. Surf. Sci. Eng.* **2020**, *14*, 288–306. [CrossRef]
12. Edenhofer, B. Physical and Metallurgical Aspects of Ionitriding. Pt. 1 and Pt. 2. In *Heat Treatment Metals*; Wolfson Heat Treatment Centre: Birmingham, UK, 1974.
13. Li, C.; Georges, J.; Li, X. Active screen plasma nitriding of austenitic stainless steel. *Surf. Eng.* **2002**, *18*, 453–457. [CrossRef]
14. Li, C.; Bell, T. Sliding wear properties of active screen plasma nitrided 316 austenitic stainless steel. *Wear* **2004**, *256*, 1144–1152. [CrossRef]
15. Lin, K.; Li, X.; Tian, L.; Dong, H. Active screen plasma surface co-alloying of 316 austenitic stainless steel with both nitrogen and niobium for the application of bipolar plates in proton exchange membrane fuel cells. *Int. J. Hydrogen Energy* **2015**, *40*, 10281–10292. [CrossRef]
16. Naeem, M.; Shafiq, M.; Zaka-ul-Islam, M.; Bashir, M.I.; Díaz-Guillén, J.C.; Lopez-Badillo, C.M.; Zakaullah, M. Novel duplex cathodic cage plasma nitriding of non-alloyed steel using aluminum and austenite steel cathodic cages. *J. Alloys Compd.* **2017**, *721*, 307–311. [CrossRef]
17. Fernades, F.; Filho, E.R.; Souza, I.; Nascimento, I.; Sousa, R.; Almeida, E.; Feitor, M.; Costa, T.; Naeem, M.; Iqbal, J. Novel synthesis of copper oxide on fabric samples by cathodic cage plasma deposition. *Polym. Adv. Technol.* **2020**, *31*, 520–526. [CrossRef]
18. Morell-Pacheco, A.; Kim, H.; Wang, T.; Shiau, C.H.; Balerio, R.; Gabriel, A.; Shao, L. Ni coating on 316L stainless steel using cage plasma treatment: Feasibility and swelling studies. *J. Nucl. Mater.* **2020**, *540*, 152385. [CrossRef]
19. Da Silva, S.S.; Bottoni, R.; Gontijo, L.C.; Ferreira, S.O. Plasma deposition of titanium nitride thin films under the effect of hollow cathode length in cathodic cage. *Matéria* **2017**, *22*, 1–12.
20. Podgornik, B.; Vižintin, J.; Wänstrand, O.; Larsson, M.; Hogmark, S.; Ronkainen, H.; Holmberg, K. Tribological properties of plasma nitrided and hard coated AISI 4140 steel. *Wear* **2001**, *249*, 254–259. [CrossRef]
21. Sprute, T.; Tillmann, W.; Grisales, D.; Selvadurai, U.; Fischer, G. Influence of substrate pre-treatments on residual stresses and tribo-mechanical properties of TiAlN-based PVD coatings. *Surf. Coat. Technol.* **2014**, *260*, 369–379. [CrossRef]
22. De Las Heras, E.; Egidi, D.A.; Corengia, P.; González-Santamaría, D.; García-Luis, A.; Brizuela, M.; López, G.A.; Martinez, M.F. Duplex surface treatment of an AISI 316L stainless steel; microstructure and tribological behaviour. *Surf. Coat. Technol.* **2008**, *202*, 2945–2954. [CrossRef]
23. Bashir, M.I.; Shafiq, M.; Naeem, M.; Zaka-ul-Islam, M.; Díaz-Guillén, J.C.; Lopez-Badillo, C.M.; Zakaullah, M. Enhanced surface properties of aluminum by PVD-TiN coating combined with cathodic cage plasma nitriding. *Surf. Coat. Technol.* **2017**, *327*, 59–65. [CrossRef]
24. Sousa, R.R.M.D.; Moura, Y.J.L.; Sousa, P.A.O.D.; Medeiros Neto, J.Q.; Costa, T.H.D.C.; Alves Junior, C. Nitriding of AISI 1020 steel: Comparison between conventional nitriding and nitriding with cathodic cage. *Mater. Res.* **2014**, *17*, 708–713. [CrossRef]
25. Barbosa, M.G.C.; Viana, B.C.; Santos, F.E.P.; Fernandes, F.; Feitor, M.C.; Costa, T.H.C.; Naeem, M.; Sousa, R.R.M. Surface modification of tool steel by cathodic cage TiN deposition. *Surf. Eng.* **2021**, *37*, 334–342. [CrossRef]
26. Diaz-Guillen, J.C.; Naeem, M.; Acevedo-Davila, J.L.; Hdz-Garcia, H.M.; Iqbal, J.; Khan, M.A.; Mayen, J. Improved Mechanical Properties, Wear and Corrosion Resistance of 316L Steel by Homogeneous Chromium Nitride Layer Synthesis Using Plasma Nitriding. *J. Mater. Eng. Perform.* **2020**, *29*, 877–889. [CrossRef]
27. Araujo, A.G.F.; Naeem, M.; Araujo, L.N.M.; Costa, T.H.C.; Khan, K.H.; Díaz-Guillén, J.C.; Iqbal, J.; Liborio, M.S.; Sousa, R.R.M. Design, manufacturing and plasma nitriding of AISI-M2 steel forming tool and its performance analysis. *J. Mater. Res. Technol.* **2020**, *9*, 14517–14527. [CrossRef]
28. Moreno-Bárcenas, A.; Alvarado-Orozco, J.M.; Carmona, J.G.; Mondragón-Rodríguez, G.C.; González-Hernández, J.; García-García, A. Synergistic effect of plasma nitriding and bias voltage on the adhesion of diamond-like carbon coatings on M2 steel by PECVD. *Surf. Coat. Technol.* **2019**, *374*, 327–337. [CrossRef]
29. Serna, M.M.; Rossi, J.L. MC complex carbide in AISI M2 high-speed steel. *Mater. Lett.* **2009**, *63*, 691–693. [CrossRef]
30. Alves, C., Jr.; De Araújo, F.O.; Ribeiro, K.J.B.; Da Costa, J.A.P.; Sousa, R.D.; De Sousa, R.S. Use of cathodic cage in plasma nitriding. *Surf. Coat. Technol.* **2006**, *201*, 2450–2454. [CrossRef]
31. Saeed, A.; Khan, A.W.; Jan, F.; Abrar, M.; Khalid, M.; Zakaullah, M. Validity of "sputtering and re-condensation" model in active screen cage plasma nitriding process. *Appl. Surf. Sci.* **2013**, *273*, 173–178. [CrossRef]
32. Hubbard, P.; Partridge, J.G.; Doyle, E.D.; McCulloch, D.G.; Taylor, M.B.; Dowey, S.J. Investigation of nitrogen mass transfer within an industrial plasma nitriding system I: The role of surface deposits. *Surf. Coat. Technol.* **2010**, *204*, 1145–1150. [CrossRef]
33. Gallo, S.C.; Dong, H. On the fundamental mechanisms of active screen plasma nitriding. *Vacuum* **2009**, *84*, 321–325. [CrossRef]
34. Fraczek, T.; Ogorek, M.; Skuza, Z.; Prusak, R. Mechanism of ion nitriding of 316L austenitic steel by active screen method in a hydrogen-nitrogen atmosphere. *Int. J. Adv. Manuf. Technol.* **2020**, *109*, 1357–1368. [CrossRef]
35. Rad, H.F.; Amadeh, A.; Moradi, H. Wear assessment of plasma nitrided AISI H11 steel. *Mater. Des.* **2011**, *32*, 2635–2643.

36. Hoshiyama, Y.; Chiba, K.; Maruoka, T. Effect of Active Screen Plasma Nitriding on Mechanical Properties of Spheroidal Graphite Cast Iron. *Metals* **2021**, *11*, 412. [CrossRef]
37. Zhang, F.; Yan, M. Microstructure and wear resistance of in situ formed duplex coating fabricated by plasma nitriding Ti coated 2024 Al alloy. *J. Mater. Sci. Technol.* **2014**, *30*, 1278–1283. [CrossRef]